Pramana – J. Phys. (2018) 91:22
https://doi.org/10.1007/s12043-018-1594-1

Characterisation of electric discharge in hollow electrode Z-pinch device by means of Rogowski coils

M S ASER[1], M E ABDEL-KADER[2], A M SHAGAR[2], H A ELTAYEB[2], H A ALGAMAL[2] and M A ABD AL-HALIM[1,*]

[1]Physics Department, Faculty of Science, Benha University, Benha 13518, Egypt
[2]Plasma and Nuclear Fusion Department, N.R.C., Egyptian Atomic Energy Authority, Inshaas 13759, Abu Zaabal, Egypt
*Corresponding author. E-mail: mohamed.abdalhalim@fsc.bu.edu.eg

MS received 12 June 2017; revised 1 December 2017; accepted 16 January 2018; published online 29 June 2018

Abstract. The hollow electrode Z-pinch (HEZP) is expressed as a new shape of Z-pinch devices in which one of the electrodes is ring-shaped. The periodic time of the discharge current is 35 μs with a total system inductance of 288 nH, total system resistance of 14 mΩ, and 34% deposited energy for a charging voltage of 8 kV. The pinch effect appears in the shape of a sharp spike in the signal of the discharge voltage and dip in the signal of discharge current, which leads to an increase in the plasma inductance at the pinch time. The plasma current density, which is measured using miniature Rogowski coil for 8 kV charging voltage and 1 torr pressure, has a maximum value of 12.1 kA/cm^2 near the axis of the discharge tube and decreases toward the wall. The helium gas pressure in the range of 1–2 torr expresses the situation of the maximum current density. The pinch time increases by increasing the gas pressure and also by decreasing the charging voltage leading to a decrement of the peak discharge current and hence the magnetic field is also decreased. A delay time of at least 4.1 μs is found to be required to form the pinch for the implemented set-up of anode–cathode dimensions and interdistance. The calculated sheath velocity is in the range of 1.2–6 cm/μs which is directly proportional to the charging voltage and inversely proportional to the gas pressure.

Keywords. Hollow electrode; Z-pinch; Rogowski coils; plasma current density; pinch time; radial velocity.

PACS No. 52.58.Lq

1. Introduction

Z-pinch devices are classified and strongly discussed by Haines in 2011 [1]. The plasma is magnetically confined in the radial direction where the discharge current J_z passes in the axial direction and induces azimuthal magnetic field B_θ, creating Lorentz force $(J_z \times B_\theta)_r$ in the inward radial direction [1]. The induced magnetic field resulting from the plasma current is associated with the Lorentz force $J \times B$ that is responsible for the pinch effect [2].

Z-pinches are considered as efficient sources of X-rays [3–5]. The pinch could be formed by applying a large potential to a wire connecting two electrodes so that the wire is vapourised and ionised and then the pinch is created [6]. Conical arrays are used to control the plasma implosion direction to produce the X-rays [7]. A 100 kJ Z-pinch device with 4 MA discharge current was used with short rise time and plasma temperature of 55 eV to produce maximum X-ray yield [8].

The plasma current density can be evaluated by using the magnetic probe depending on the space and time variation of the magnetic field [9]. A miniature Rogowski coil has been used to measure the plasma current density [10] and the results showed that the plasma current density decreases with radial distance [9,11]. Many forms of linear Z-pinch devices have been constructed like a linear Z-pinch with two hollow electrodes, where the pinch time and its radius were evaluated and the current density was determined from the magnetic field as a function of time, radius, and the velocity of the imploding plasma layer [12]. Decreasing the gas pressure shifts the pinch towards to the peak of the discharge current and it also increases the pinch current which flows through the plasma column [13].

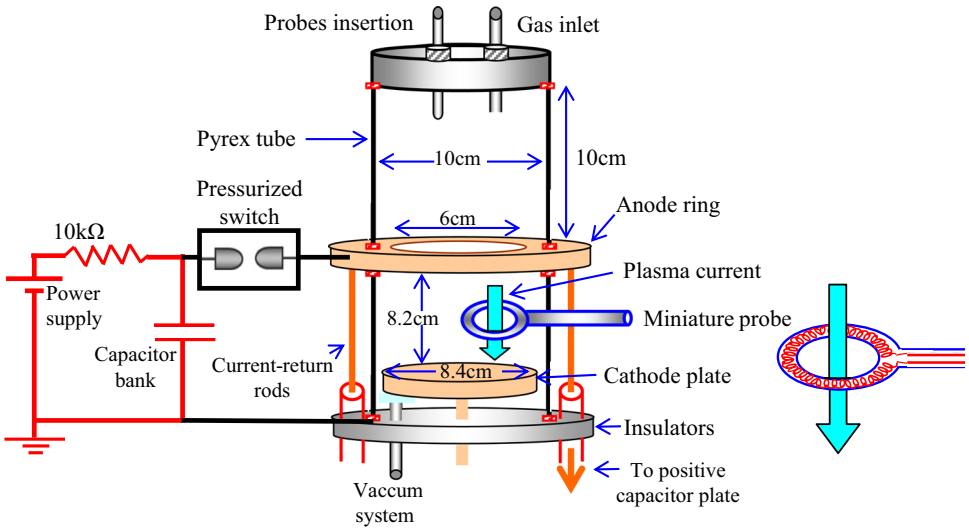

Figure 1. Schematic diagram of the HEZP device and electric circuit.

The results showed that the pinch time and pinch duration decrease with increasing voltage [14]. By decreasing the gas pressure, the current sheath moves faster so that the pinch time is reduced [13,15]. The same effect of the high pressure and heavier gas molecular weight on the pinch duration and the sheath velocity is observed in many experiments [16–19] and are also obtained theoretically by Lee's model [20,21]

In the present experiment, the pinch effect will be studied in a new Z-pinch construction using hollow electrode to allow sheath expansion in the axial direction. The discharge current and voltage will be measured using Rogowski coil and potential divider respectively. A miniature Rogowski coil will be used to measure the plasma current density and the pinch time under different charging voltages and helium gas pressures.

2. Experimental set-up

The discharge chamber of the HEZP is described in [21]. Figure 1 shows a schematic diagram of the HEZP device and the electric circuit. It consists of two cylindrical Pyrex tubes of 10 cm diameter, 10 cm length, and two copper electrodes. The upper electrode is hollow, of 6 cm diameter, and is fixed between the lower discharge tube and the higher expansion tube. The discharge occurs first in the lower tube, and then it is propelled towards the upper one which is considered as the expansion tube. The lower electrode is an 8.4 cm diameter plate cathode. The two electrodes are separated by 8.2 cm. Eight isolated copper rods were used as current-return rods to reduce the total inductance of the circuit. These rods are connected to the anode and surround the lower tube. The discharge occurs by discharging 108 μF condenser bank with a maximum stored energy of 5.4 kJ. Helium gas was used in this study at different pressures up to 10 torr.

Rogowski coil is one of the main diagnostic tools that is used in most of the pinch experiments [22,23]. It is used in the present work to measure the main discharge current and the plasma current density. The first coil is used outside the chamber to measure the total discharge current. The second coil is the miniature Rogowski coil which works as a probe to measure plasma current which passes inside the chamber. The coil is allowed to move in the radial direction so that plasma current density can be measured in different radial distances from the axis centre to the wall.

The outer Rogowski coil which is used to measure the discharge current, has 120 turns, 3.25 cm major radius, and a single turn radius of 0.35 cm. The circuit integrator has a resistance of 100 kΩ and a capacitance of 10 nF. The bandwidth limits of the coil are 1×10^3 kHz and 2.8×10^9 Hz, which satisfy the integrator condition for the experiment in the case of discharge current of 35 μs periodic time. On the other hand, the miniature coil has 100 turns, a major radius of 0.53 cm, and a single turn radius of 0.1 cm, and so the bandwidth limits are 1.67×10^4 kHz and 2.6×10^8 Hz which are also suitable for the experiment.

3. Plasma sheath dynamics in HEZP

In the HEZP device, the axial discharge current, J_z, will induce azimuthal magnetic field, B_θ, so that Lorentz force F_r will be generated in the radial direction and confines the plasma sheath [24,25]. The upper electrode is a hollow one and so it allows the plasma to be expelled

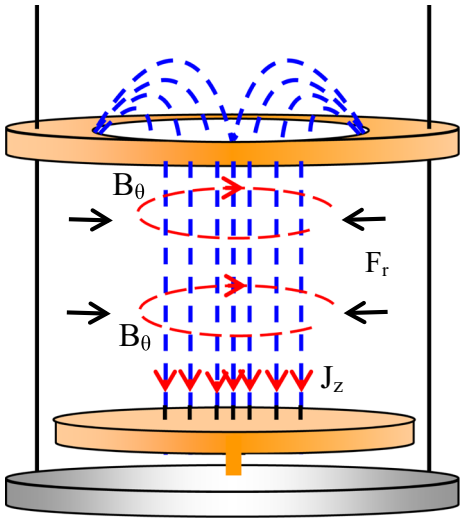

Figure 2. Schematic diagram of the plasma shape in the HEZP device.

vertically. Lorentz force confines the plasma sheath in the radial direction and allows for the sheath expansion towards the upper hollow electrode [1,21,26].

When applying a sufficient electric potential, discharge occurs and cylindrical sheath of plasma is created between the lower plate and the upper hollow electrodes, as shown in figure 2. An azimuthal magnetic field B_θ will be induced so that the generated Lorentz force will confine the plasma towards the axis of the chamber and form the pinch and could be expelled vertically towards the expansion chamber, throw the hollow electrode [14,27] as an electromagnetic propulsion [28,29]. The confined plasma sheath which is formed at the lower chamber forms a plasma column which could be propelled towards the upper chamber. A dip is clearly appeared in the discharge current signal accompanied by a sharp spike in the voltage signal [14].

4. Experimental results

4.1 *Discharge current and voltage*

Figure 3 shows a simple waveform of the discharge current and discharge voltage signals. The discharge current $I_{\rm dis}$ is measured using Rogowski coils with integrator circuit while a calibrated potential divider is used for measuring the discharge voltage.

The discharge current reaches a maximum value at about 7 μs. The figure shows a voltage spike and discharge current dips at about 5.0 μs to 5.25 μs which means that a pinch is created. The peak of the discharge current can be calculated theoretically by using the relation

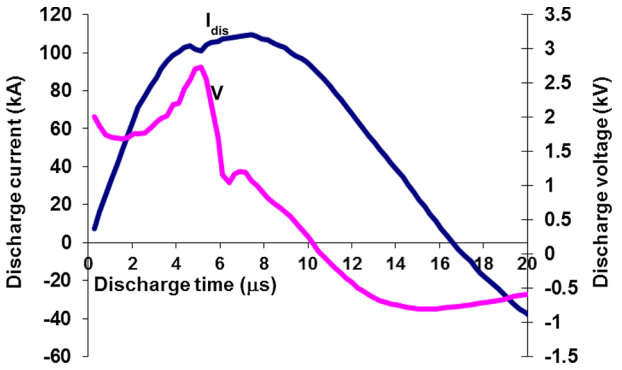

Figure 3. A sample of the pinch effect appearing in the signal waveform of both the discharge current and discharge voltage for 8 kV charging voltage.

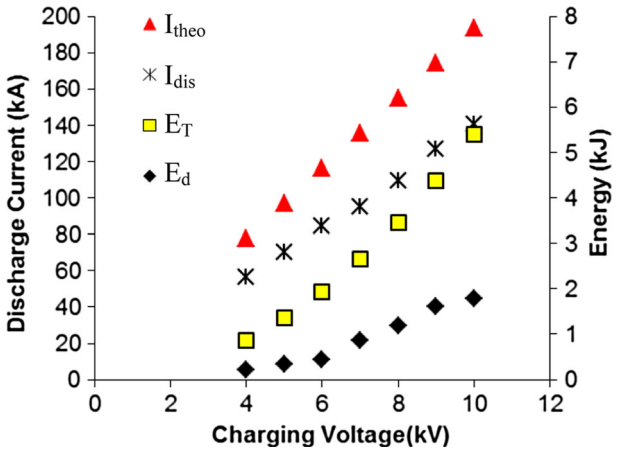

Figure 4. The discharge current and the energy as a function of the charging voltage.

$$I_{\rm theo} = \frac{2\pi C_{\rm ch} V_{\rm ch}}{\tau}, \tag{1}$$

where $C_{\rm ch} = 108\ \mu$F is the capacitance of the condenser bank, $V_{\rm ch}$ is the charging voltage, and $\tau = 35\ \mu$s is the periodic time of the discharge current. Figure 4 shows the relation between both the calculated and experimental discharge current vs. the charging voltage at $P = 1$ torr. This figure shows also the relation between both the total stored energy $E_{\rm T}$ of the main condenser bank, which is equal to $\frac{1}{2} C_{\rm ch} V_{\rm ch}^2$, and the deposited energy $E_{\rm d}$ which is obtained by integrating the discharge power $P_{\rm dis}$ according to the relation

$$E_{\rm d} = \int P_{\rm dis} {\rm d}t = \int I_{\rm dis} V_{\rm dis}\ {\rm d}t. \tag{2}$$

The maximum calculated power is 260 MW while the deposited energy is 1.27 kJ which is about 34% of the total stored energy for 8 kV charging voltage. The difference between the total storage energy and the deposited energy is exhausted by the circuit resistance and ionisation of neutral particles of the gas. The total

circuit inductance can be calculated from the resonance condition in the R–L–C circuit as

$$L_{\mathrm{T}} = \frac{\tau^2}{4\pi^2 C_{\mathrm{ch}}}. \tag{3}$$

The calculated value of total L_{T} is 288 nH. The total circuit resistance R_{T} is calculated from the instantaneous current $I(t)$ flowing through the circuit which is given by [30]

$$I(t) = I_0 \sin(\omega t) \exp(-R_{\mathrm{T}} t/2L_{\mathrm{T}}). \tag{4}$$

At the peak current I_{p} $\sin(\omega t) = 1$ so that

$$\ln \frac{I_{\mathrm{p}}}{I_0} = -\frac{R_{\mathrm{T}}}{2L_{\mathrm{T}}} t \tag{5}$$

so that the total circuit resistance R_{T} can be calculated from the relation between $\ln I_{\mathrm{p}}$ and the discharge time. The total circuit resistance is 14 mΩ at 8 kV charging voltage and $P = 1$ torr. This value indicates that the total circuit resistance is small compared to the circuit impedance.

4.2 *Plasma current density*

A miniature Rogowski coil has been used to measure the plasma current density. It is inserted radially inside the plasma bulk and connected to an integrator circuit. The output signal had been calibrated so that the current density J is given as a function of the output voltage V_{out} according to the equation

$$J(\mathrm{A.cm}^{-2}) = \mathrm{Const.} \times V_{\mathrm{out}}(\mathrm{V}),$$

$$\mathrm{Const.} = 5.74 \times 10^4 (\Omega^{-1}\,\mathrm{cm}^{-2}). \tag{6}$$

Figures 5a–5c show the signal waveforms for plasma current at different helium gas pressures. We assume that the plasma current is perpendicular to the surface of the major area of Rogowski coil plane. The decrease in the discharge current at the pinch point is referred to as a compression of the plasma sheath in which the magnetic pressure exceeds the kinetic pressure of the ionised gas, which finally leads to a compression which increases the plasma inductance and reduces the discharge current [14]. In the absence of further diagnostic tools, the hypothesis for interpreting the experimental results is that, the kinetic pressure and magnetic pressure are the main reasons for plasma dynamics and pinch formation.

Figure 5 indicates that the plasma current density is the highest for intermediate pressure (figure 5b) and that a multipinch can take place for lower pressures (figure 5a). The experimental measurements indicate that a current filamentation may occur, but the recorded signals recommended a multipinching process. The peak

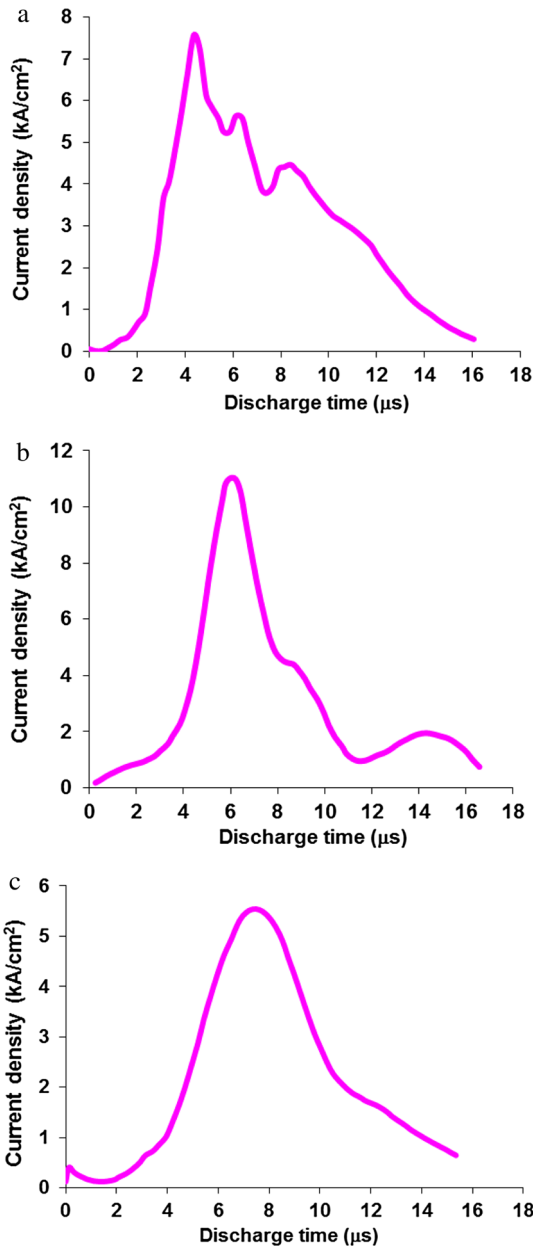

Figure 5. The variation of plasma current signals at the axis for (**a**) 0.25 torr, (**b**) 2 torr, and (**c**) 10 torr.

maximum of the plasma current synchronises the time of the pinch at the discharge current dip. This time increases with the increase in gas pressure due to the heavier sheath.

Figure 6 shows that the plasma current density increases with increase in the charging voltage due to higher peak discharge current which increases the ionisation inside the chamber. Increasing the charging voltage mainly enhances the current delivery and this in turn increases the magnetic field and hence characteristic parameters like plasma current density increases. For a charging voltage of 6 kV or less, the plasma current

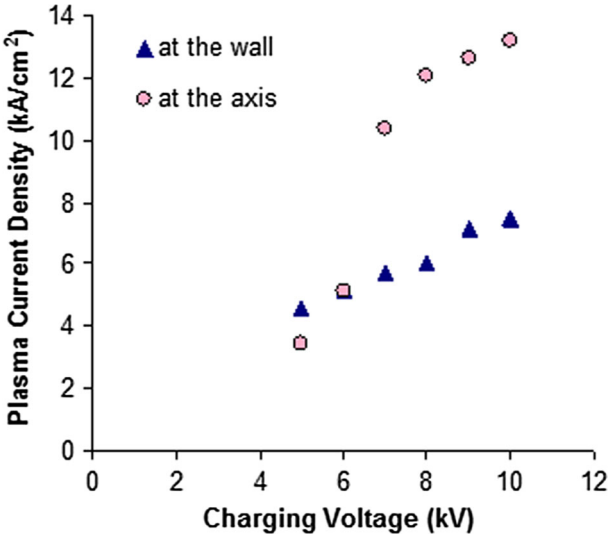

Figure 6. The plasma current density as a function of the charging voltage for helium gas pressure of 1 torr.

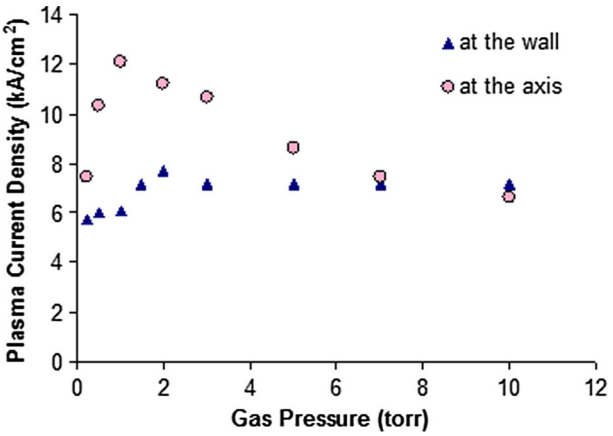

Figure 7. The plasma current density as a function of helium gas pressure for $V = 8$ kV.

density at the axis of the discharge tube is low compared to that at the wall which can be attributed to the weak confinement.

Figure 7 shows the variation of plasma current density, measured at the axis and near the wall as a function of helium gas pressure. The figure shows that the plasma current density at the axis of the discharge tube is higher than that near the wall which is similar to that in figure 6. It also shows that the plasma current density near the wall has a maximum value of about 7.8 kA/cm^2 for 2 torr pressure while at the axis, the plasma current density has a maximum value of about 12.1 kA/cm^2 for 1 torr pressure.

One can differentiate between two parts in this figure around a critical pressure synchronously with the maximum plasma current. On the left-hand side, the plasma current density decreases by decreasing the gas

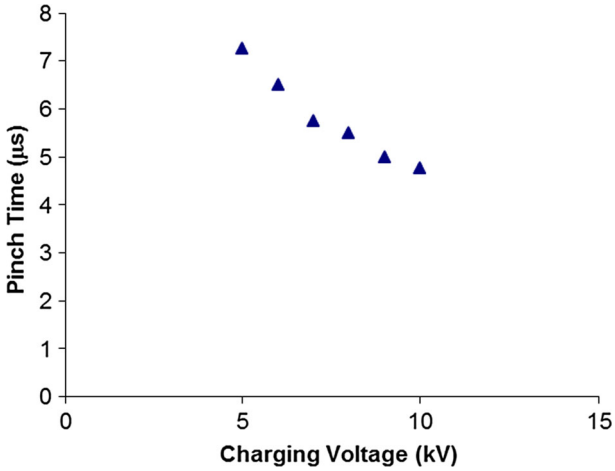

Figure 8. The variation of pinch time with charging voltage at the wall for $P = 1$ torr.

pressure. This can be attributed to the fact that most of the plasma sheath can be propelled axially towards the expansion chamber through the ring electrode. Also, for lower pressure, better confinement occurs with shorter pinch radius. This will increase the plasma sheath speed and reduce the current due to the higher dynamic resistance, i.e. increase the inductance which takes place for higher confinement with the narrower pinch area [31].

At the right-hand side of this curve, the plasma current density decreases by increasing the gas pressure. For high pressure, the confinement is more difficult; the higher kinetic pressure increases the pinch radius so that the area through which the current passes is wide and the current density is low. The propulsion in the axial direction is reduced as well due to the weaker confinement. This behaviour is similar to the trend of the neutron yield variation with the gas pressure [2,32] in which beyond a certain value of the gas pressure, increase or decrease of the pressure does not allow the pinch to occur at the same time of discharge current peak [32].

4.3 *Pinch time*

The pinch time (t_p) is defined as the time of the pinch formation which starts from the gas breakdown [32]. It is considered as the time of dip appearing in the current trace or the minimum value in the derivative trace [14,33,34]. Figure 8 shows that the pinch time decreases by increasing the applied voltage at a constant pressure of 1 torr and the same trend was observed in previous researches [14,35,36]. At higher charging voltages, the discharge current is higher and so the pinch effect occurs faster, and the pinch reaches to the maximum resist of kinetic pressure faster, hence the pinch created and annihilated in a shorter time than that of a low charging voltage.

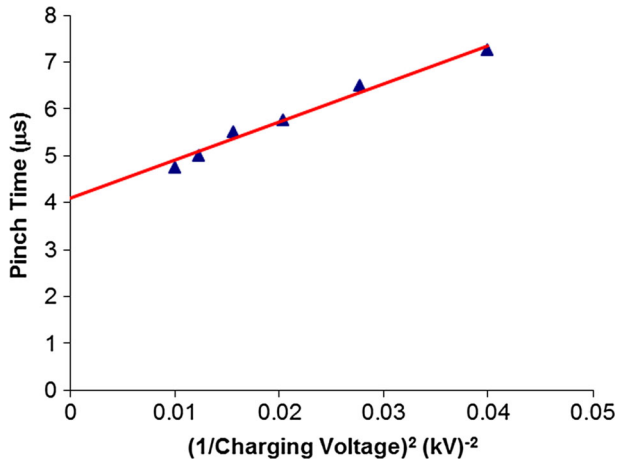

Figure 9. Relation between the pinch time and $(1/\text{charging voltage})^2$.

Figure 9 shows that the pinch time is inversely proportional to the square of the charging voltage. The fitting of this relation is given in the form of a linear equation, $t_p = \text{Const.} \times (1/V^2) + t_d$, where $t_d = 4.1\ \mu$s and is considered to be the minimum time required to create the sheath before moving and creating the pinch whatever is the value of the charging voltage [34]. The value of t_d indicates that, whatever is the value of the applied charging voltage, a time of at least 4.1 μs is required for the pinch to occur for the implemented set-up of anode–cathode dimensions and interdistance. This is the time needed for gas ionisation and magnetic compression inward to the axis of the chamber [14]. The breakdown phase always occurs before the sheath motion in the radial direction. The breakdown consumes a fraction of the discharge time to create the plasma sheath [37–39].

Going back to figure 5, one can see that the pinch time is shorter for lower gas pressures [32]. It is also shown that the lower pressures allow a multipinch generation. Figure 10 shows that the pinch time, which is measured near the wall, increases with increase in gas pressure for 8 kV charging voltage. The heavy sheath which is formed in the case of higher pressures reduces the sheath velocity and increases the time required for the pinch creation. Also, increasing the gas pressure exhausts part of the energy to ionise the neutral atoms of the gas, leaving the heavy sheath with less energy to be used in confinement.

4.4 *Plasma sheath velocity*

The values of t_p and t_d can be used to calculate the average radial plasma sheath velocity. This velocity is given by dividing the electrode radius by $\Delta t = (t_p - t_d)$ which is the real time of motion [34]. Figure 11 shows that the radial velocity increases by increasing the

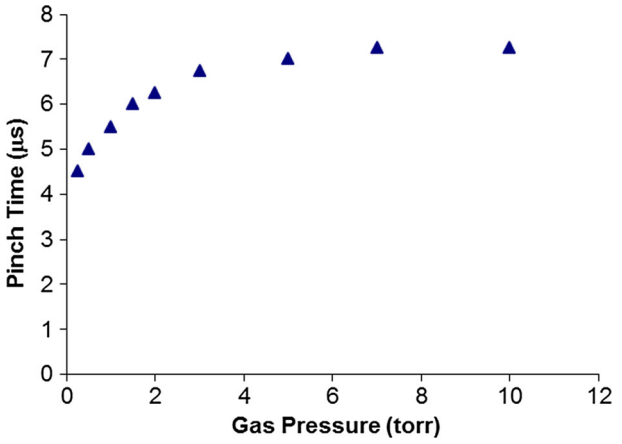

Figure 10. The variation of the pinch time with gas pressure at the wall for 8 kV charging voltage.

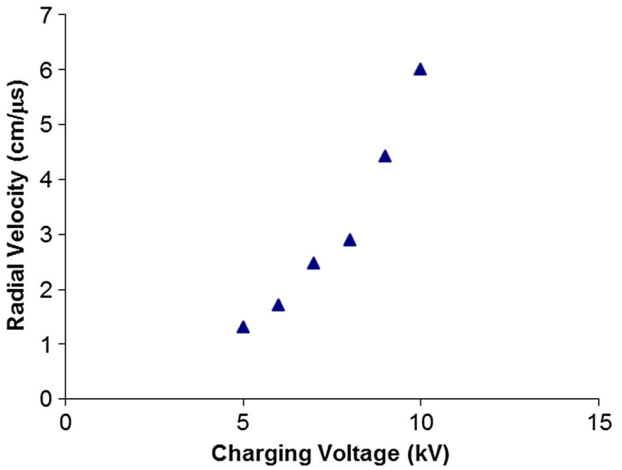

Figure 11. The radial velocity as a function of charging voltage when the helium gas pressure is 1 torr.

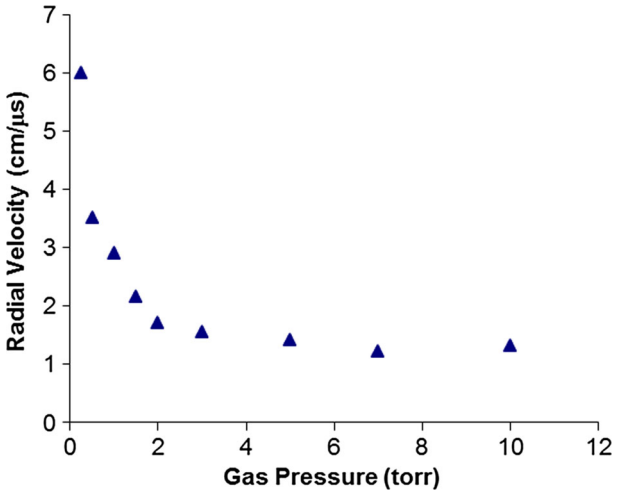

Figure 12. The radial velocity as a function of gas pressure for 8 kV charging voltage.

charging voltage as a result of increase in the discharge current and hence the magnetic pressure. The relation is almost exponential and the radial velocity is in the range between 1.3 and 6 cm/μs for charging voltages of 5 kV and 10 kV respectively.

Using the same method used previously for velocity calculations, the radial velocity can be obtained as a function of helium gas pressure. Figure 10 shows that the curve intercepts with the vertical axis when pinch time = 4.1 μs which is the same as in figure 9. It is observed in figure 12 that the radial velocity decreases by increasing the gas pressure because the mass of the plasma sheath is heavier and the pinch needs longer time to occur. The velocity for 8 kV charging voltage and 1 torr pressure is about 2.9 cm/μs.

5. Conclusion

The hollow electrode Z-pinch (HEZP) is a new design of linear pinch devices in which the hollow electrode was used to allow for plasma sheath propulsion due to the confinement process. The pinch effect appeared as a dip in the discharge current and a spike in the discharge voltage. The deposited energy was about 34% of the total stored energy for 8 kV charging voltage.

A miniature Rogowski coil connected with integrator circuit was used to measure the plasma current density at the axis and the wall. The peak plasma current density increases by increasing the charging voltage which leads to an increase in the peak discharge current and hence the magnetic field is also increased. The current density is maximum for gas pressures between 1 torr and 2 torr. The heavy sheath for higher pressures reduces the confinement, increases the pinch time, and reduces the sheath velocity. On the other hand, reducing the gas pressure to values less than 1 torr gives more chance for plasma to be propelled towards the expansion chamber before annihilation, reduces the pinch time due to the light sheath of high velocity. Also, a multipinch effect was detected in the case of lower pressures rather than higher pressures.

It was shown that a delay time of at least 4.1 μs was required to form the pinch for the implemented set-up of anode–cathode dimensions and interdistance. The calculated sheath velocity is directly proportional to the charging voltage and inversely proportional to the gas pressure. The sheath velocity was found to be in the range between 1.3 and 6 cm/μs while the average velocity for 1 torr pressure and 8 kV charging voltage is about 2.9 cm/μs.

Future study includes experimental investigation of the plasma behaviour in the HEZP for different chamber dimensions of different electrode materials and cathode shape which affects electromagnetic propulsion through the hollow anode. Also, measurements of the axial plasma sheath velocity as well as the magnetic field distributions in different radial and axial distances will be included.

References

[1] M G Haines, *Plasma Phys. Control. Fusion* **53**, 093001 (2011)
[2] C Moreno, H Bruzzone, J Martinez and A Clausse, *IEEE Trans. Plasma Sci.* **28**, 1735, (2000)
[3] R A Vesey, M C Herrmann, R W Lemke, M P Desjarlais, M E Cuneo, W A Stygar, G R Bennett, R B Campbell, P J Christenson, T A Mehlhorn, J L Porter and S A Slutz, *Phys. Plasmas* **14**, 056302 (2007)
[4] M K Matzen, *Phys. Plasmas* **4**, 1519 (1997)
[5] M E Cuneo *et al*, *Phys. Plasmas* **8**, 2257 (2001)
[6] M G Haines, S V Lebedev, J P Chittenden, F N Beg, S N Bland and A E Dangor, *Phys. Plasmas* **7**(**5**), 1672 (2000)
[7] V V Aleksandrov, E V Grabovski, A N Gribov, A N Gritsuk, S F Medovshchikov, K N Mitrofanov and G M Oleinik, *Plasma Phys. Rep.* **35**(**2**), 136 (2009)
[8] V D Selemir, *Plasma Phys. Rep.* **33**(**5**), 381 (2007)
[9] R G Jahn and W Von Jaskowsky, *AIAA J.* **2**, 1749 (1964)
[10] E Torbert, I Furno, T Intrator and E Hemsing, *Rev. Sci. Instrum.* **74**, 5097 (2003)
[11] S H Ishii, T Hara, F Sonoda, M Fukuta and I Hayashi, *Elect. Eng. Jap.* **106**(**3**), 487(1986)
[12] F Dothan, H Riege, E Boggasch and K Frank, *J. Appl. Phys.* **62**, 3585 (1987)
[13] Sh Al-Hawat, M Akel and S Lee, *J. Fusion Energy* **30**, 494 (2011)
[14] M E Abdel-kader, M A Abd Al-Halim, A M Shagar, H A Eltayeb, H A Algamal and A H Saudy, *J. Fusion Energy* **33**, 53 (2014)
[15] H Bruzzone, A Clausse, M Barbaglia and H Acuna, *Plasma Phys. Control. Fusion* **54**, 012001 (2012)
[16] Y P Zhao, S Jiang, Y Xie and Q Wang, *Appl. Phys. B* **99**, 535 (2010)
[17] M Akel and S Lee, *J. Fusion Energy* **32**, 111 (2013)
[18] M Akel, S Lee and S H Saw, *IEEE Trans. Plasma Sci.* **40**(**12**), 3290 (2012)
[19] S Lee, S H Saw, L Soto, S V Springham and S P Moo, *Plasma Phys. Control. Fusion* **51**, 075006 (2009)
[20] M N Sharak, S Goudarzi, A Raeisdana and M Jafarabadi, *J. Fusion Energy* **32**, 258 (2013)
[21] M A Abd Al-Halim and M S Afify, *Eur. Phys. J. D* **57**, **71** (2017)
[22] A Kanani, M N Nasrabadi, B Shirani and I Jabbari, *Pramana – J. Phys.* **85**(**1**), 149 (2015)
[23] M Z Khan, L K Lim, S L Yap and C S Wong, *Pramana – J. Phys.* **85**(**6**), 1207 (2015)
[24] Z Ali, S Lee, F D Ismail, Saktioto, J Ali and P P Yupapin, *Procedia Eng.* **8**, 393 (2011)

[25] Marek J Sadowski and Marek Scholz, *Nucleonika* **57**, 11 (2012)
[26] K T Lee, S H Kim, D Kim and T N Lee, *Phys. Plasmas* **3**, 1340 (1996)
[27] T E Markusi, K A Polziny, J Z Levinez, C A McLeaveyx and E Y Choueiri, *AIAA J.* **17**, 3257 (2000)
[28] M Keidar, I D Boyd, N Lepsetz, Th E Markusic, K A Polzin and E Y Choueiri, *37th AIAA/ASME/SAE/ASEE Joint Propul. Conf.* (Salt Lake City, UT, July 8–11, 2001) AIAA 2001-3898
[29] P C Sleziona, M Auweter-Kurtz and H O Schrade, *Proc. 23rd IEPC* (Seattle, WA, USA, 1993) p. 609
[30] R A Serway and J W Jewett, *Physics for scientists and engineers with modern physics,* 8th edn (Brooks/Cole, Belmont, CA, 2010)
[31] S Lee, *Appl. Phys. Lett.* **95**, 151503 (2009)
[32] R Verma, R S Rawat, P Lee, A T L Tan, H Shariff, G J Ying, S V Springham, A Talebitaher, U Ilyas and A Shyam, *IEEE Trans. Plasma Sci.* **40**(**12**), 3280 (2012)
[33] F Veloso, C Pavez, J Moreno, V Galaz, M Zambra and L Soto, *J. Fusion Energy* **31**, 30 (2012)
[34] M E Abdel-kader, M A Abd Al-Halim, A M Shagar and A H Saudy, *Eur. Phys. J. D* **68**, 160 (2014)
[35] D G Fearn and E R Wooding, *Brit. J. Appl. Phys.* **18**, 213 (1967)
[36] M Emami, *Laser Phys.* **17**(**1**), 1, (2007)
[37] A Donges, G Herziger, H Krompholz, F Ruhl and K Schonbach, *Phys. Lett. A* **76**, 391 (1980)
[38] M Mathuthu, T G Zengeni and A V Gholap, *IEEE Trans. Plasma Sci.* **25**, 1382 (1997)
[39] H Schmidt, *Nucleonika* **46**, 15 (2001)